Ultrasonic Monitoring of the Seal Quality in Flexible Food Packages

AYHAN OZGULER[1], SCOTT A. MORRIS[2*], *and* WILLIAM D. O'BRIEN, JR.[3]

[1]*Department of Food Science & Human Nutrition*
University of Illinois

[2]*Departments of Food Science & Human Nutrition*
and Agricultural Engineering
University of Illinois
1304 W. Pennsylvania Avenue, AESB: 382
Urbana, IL 61801

[3]*Department of Electrical and Computer Engineering*
University of Illinois

Ultrasonic Backscattered Amplitude Integral (BAI) values are used to detect critical and major defects such as nonbonding, wrinkles and bubbles distributed within the seal area of flexible food packages. The BAI-mode imaging by itself is not capable of detecting such nonbonding, wrinkles and bubbles distributed within the seal area. For this study, model defects in the seal region of all-plastic and foil-containing films were created by varying the sealing-bar temperature. Seal regions were scanned by a 17.3-MHz ultrasonic transducer, and the waveform for each scan point was processed by the BAI-mode method. The mean and the coefficient of variation of the BAI values (BAICV) were calculated. It is shown that a combination of mean BAI value and BAICV value can detect defects distributed in seals in flexible food packages. This technique has the potential of providing a real-time, on-line control by sensing whether a proper seal has been achieved.

INTRODUCTION

The food industry continues to pursue better containers that are inexpensive, attractive, and easy to transport and store. With the accelerated changes occurring in packaging technology, non-traditional shelf-stable packaging, such as retortable pouches and trays, is being considered as replacement for the production volume occupied by canning. Such flexible food packages offer the consumer cheap, lightweight, durable and easy-to-open packaging (1–5). These packages provide food preservation superior to that provided by traditional cans and glass containers (6–10).

Sealing is the critical step in the use of flexible food packages because post-process contamination of processed foods is mostly linked to seal and package integrity issues (11–15). The National Food Processors Association (NFPA) states that critical defects such as channel leakers and nonbonding in the seal area of flexible food packages could result in a potential public health problem (16). If package content is contaminated in any production lot during packaging or storage, the NFPA recommends a thorough inspection to ensure that no containers with lost hermetic seals are distributed.

Most post-seal quality control is based on time-consuming, expensive destructive and nondestructive examinations. Currently, quality control is mainly performed by post production inspection. This results in high scrap rates with destructive techniques (17) and low detection rates with nondestructive visual (human) inspection techniques due to low human ocular resolution (~50μm) (18). On-line quality control in automated thermal fusion and bonding operations may provide higher productivity, lower costs and greater package reliability.

Thermal fusion and bonding, the predominant method of sealing flexible plastic and coated paper

*Corresponding author: smorris@uiuc.edu
This work was supported by (1) the Value-added Research Opportunities Program, Agricultural Experiment Station; and (2) Illinois Council on Food and Agricultural Research (C-FAR) Competitive Grants Program, University of Illinois, Urbana.

packages, can be achieved by several methods: hot-tool welding, ultrasonic welding, RF and laser welding, dielectric welding, solvent bonding, hot-gas welding, vibration welding, infrared sealing, and induction sealing (19–28). In these methods, the crystalline structure of the polymer in the seal interface changes into liquid above the melting point of the polymer, and the interface is allowed to solidify, resulting in a weld. Three major nonmaterial factors control seal quality: the pressure of the sealing jaws, the temperature of the sealing medium, and the dwell time during when the sealing jaws press the material. In ultrasonic and vibration welding, weld time, weld pressure, and amplitude of vibration are the most important parameters (21, 22, 28). These factors are interrelated; when one of these elements is changed, the others require adjustments to provide the same seal quality.

In this study, heat sealing was used to fuse plastic packages' seal areas. To create seals of different quality, the temperature of the band sealer was varied, while keeping the pressure and the dwell time constant. Three heating schemes were used: in case I, the polymer in the seal area, i.e., polyethylene, was heated below the melting point of the polymer, then cooled; in case II, it was heated to optimal temperatures (greater than melting point), then cooled; in case III, it was overheated, then cooled. At temperatures below the melting point, the crystal structure is not completely destroyed (29), and interchain diffusion is not complete (30), which may result in incomplete bonding in the seal area after cooling the sample. At optimal temperatures above the melting point, the crystalline structure is completely melted, and no spherulites remain in the melt (31), which may provide solid interface in the seal area after the sample is cooled. At temperatures far above the melting point, polymer degradation occurs due to overheating.

The ultrasonic, pulse-echo Backscattered Amplitude Integral (BAI)-mode imaging technique was developed to detect defects nondestructively in the seal area of flexible food packages (32). This technique has the capability of detecting channel defects as small as 6 μm at a center frequency of 17.3 MHz. However, it is more effective for defects larger than 15 μm (33–38). Detection of smaller defects, with a corresponding decrease in penetration depth, is possible at higher frequencies. By being able to detect channel defects smaller than 50 μm in diameter buried in opaque material, the BAI-mode imaging method is already exceeding the reliability of human inspection. This method has the potential for being the basis of an on-line, nondestructive package seal-integrity inspection device.

This study shows that the BAI-mode imaging technique is not able to detect defects such as non-bonding, wrinkles, bubbles, and blisters distributed in the seal region. According to NFPA, nonbonding and delamination are critical defects; blisters, bubbles, and wrinkles are major defects. Critical and major defects may compromise package integrity. The objective of this study is to report on a new technique that identifies such defects and quality variation that the basic BAI-mode imaging method cannot identify.

MATERIALS AND METHODS

Sample Preparation

Two retortable pouch materials were used as samples. The material composition of the transparent all-plastic film was nylon/poly(vinylidene chloride)/polypropylene (Fuji Tokushu Shigyo Co. Ltd., Seto Aichi, Japan) with a thickness of 110 μm. The opaque material was polyester/aluminum foil/polypropylene (American National Can Company, Chicago) with a thickness of 120 μm. Polypropylene was the heat-sealing layer for both films.

Samples were produced by welding the polypropylene layers of two identical packaging materials with an automatic band sealer (Doboy HS-C42054, Doboy Co., New Richmond, Wis.). In band sealing, endless stainless steel bands (with non-stick DuPont Teflon® coating) carry the two layers of package material between heated bars to pass heat through the material. Next, the welded sample travels between a pair of air-cooled bars. The band speed of the machine was 0.083 m/s. The sealing-bar temperature was adjusted between 90 and 200°C for the all-plastic films and between 140 and 250°C for the foil-containing films, both welded at 10°C intervals.

System Description

Figure 1 shows the block diagram of the data acquisition system in which a GPIB board controlled by a program coded in C, communicated with a host PC (ZEOS 66 MHz 486), motor controllers, and a pulser-receiver. The mechanical movement of the transducer for scanning was achieved by a five-axis (three linear and two rotational axes) precision positioning system (Daedal Inc., Harrison City, Pa.). The linear and rotational positional accuracies of the system were 2 μm and 0.01°, respectively. The sample was affixed to a plastic holder and submersed in a degassed water tank (~20°C) so that its surface was approximately normal to the direction of the propagated sound beam. A pulser-receiver (Model 5800, Panametrics, Waltham, Mass.) operating in pulse/echo mode controlled by the PC was used to produce the 300 V monocycle pulse that excited a spherically focused ultrasonic transducer with nominal center frequency of 20 MHz (Model V317, Panametrics, Waltham, Mass.). However, the measured center frequency of the transducer was 17.3 MHz (39). The received echo signal was amplified (20 dB), bandpass filtered (1–35 MHz) by the pulser-receiver, and then displayed (500Ms/s) on a digitizing oscilloscope (Model 9374L, LeCroy, Chestnut Ridge, N.Y.). The PC retrieved the digitized echo waveforms from the oscilloscope, and the stored waveforms were transferred to a SUN workstation for off-line processing.

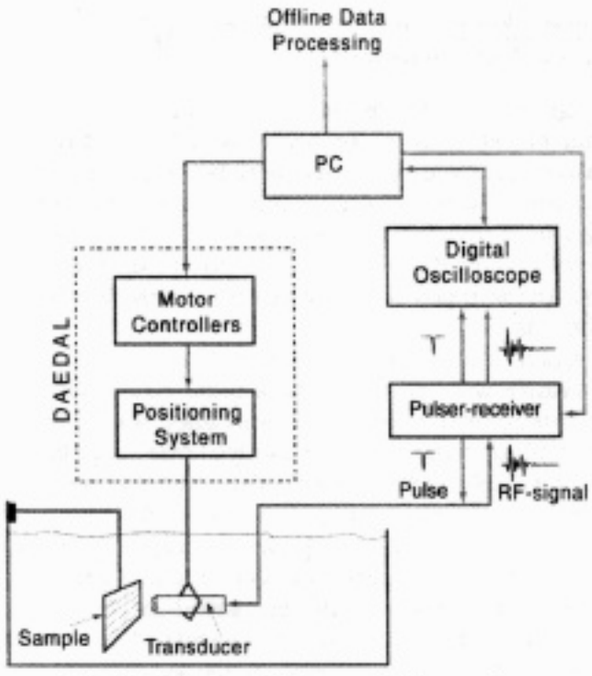

Fig. 1. Diagram of data acquisition system.

Data Acquisition

The focal length of the transducer was 12.7 mm. Therefore, the round-trip time-of-transition (TOT) for the ultrasound pulse in the water was 17.2 μs at the focus [TOT = $2 \times z/c_w$, where z is the focal length, and c_w is the speed of sound in the water, 1483 m/s at 20°C, (40)]. Radio frequency (RF) echo waveforms at each scan point were acquired and stored between TOT = 16.8 and 17.8 μs to include the sample thickness, as shown in *Fig. 2*. Each RF waveform obtained in this TOT range contained 170 data points. The four edges of the rectangular sample surface were scanned to verify that the waveforms were within the specified TOT range.

The sample was scanned in a rectangular grid pattern. The horizontal and vertical grid spacings were 200 μm and 100 μm, respectively. The horizontal direction was approximately parallel to the sealing direction. The field-of-view was 1.5 mm (vertical direction) by 10.0 mm (horizontal direction). The number of waveforms (RF echo signals) was 50 (10 mm/200 μm) in the horizontal direction and 15 (1.5 mm/100 μm) in the vertical direction for the total number of 750 (15 × 50) waveforms. The three-dimensional data set contained 750 170-point RF echo signals.

The BAI-Value Matrix and Its Coefficient of Variation

The three-dimensional data set was processed to produce the two-dimensional Backscattered Amplitude Integral (BAI)-value matrix (32, 33). Each RF echo signal was Hilbert-transformed to produce its envelope (*Fig. 2*). The echo amplitude was further integrated between TOT = 16.8 μs and 17.8 μs to obtain the BAI-value. This value was calculated for each scan point, generating a 15 × 50 BAI-value matrix. This matrix was calculated for each packaging sample.

The mean and standard deviation were calculated for each BAI-value matrix. The coefficient of variation was calculated for each packaging sample as:

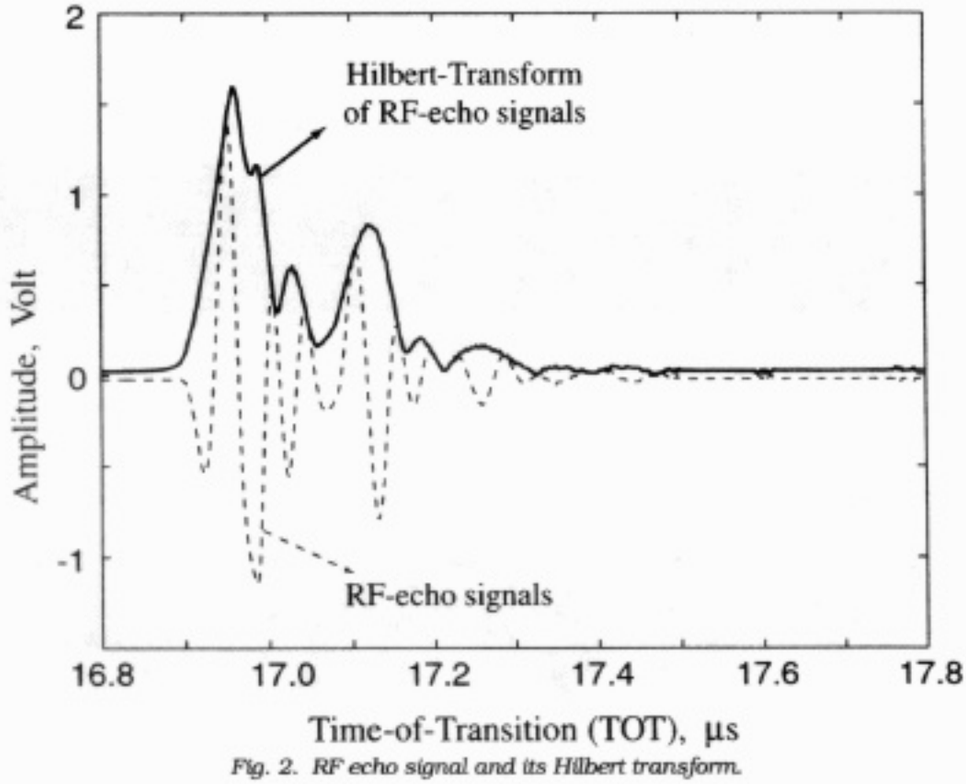

Fig. 2. RF echo signal and its Hilbert transform.

$$BAICV = \frac{\text{Standard deviation of BAI-values in the BAI-value matrix}}{\text{Mean of BAI-values in the BAI-value matrix}} \quad (1)$$

The BAICV represents the coefficient of variation of BAI-values in the BAI-value matrix.

The BAI-Mode Imaging

The BAI-mode image of each sample was generated by our previously described technique (32). Briefly, columns and rows of the BAI-value matrix were interpolated by a factor of ten (200 μm/10) and by a factor of five (100 μm/5), respectively. The interpolation resulted in pixel sizes of 20 μm × 20 μm with the number of rows and columns in the BAI-value matrix of 75 (15 by 5) and 500 (50 by 10), respectively. The normalized image matrix was used to yield a gray scale image (*Fig. 3*).

Sample Validation

A scanning laser acoustic microscope (SLAM), (Sonomicroscope 100®, Sonoscan, Inc., Bensenville, Ill.), operating at an acoustic frequency of 100 MHz, was used to examine all samples. It had been previously demonstrated that the SLAM could nondestructively image defects as small as 10 μm in diameter in plastic packages (41).

The SLAM is a through-transmission imaging system that can determine bulk wave ultrasonic properties of a thin specimen (42, 43). In addition to producing an acoustic image, the SLAM can produce an interference pattern (interferogram) (*Fig. 4*), from which the sound speed of the specimen can be determined. The interferogram consists of vertical (constant phase) interference lines, which are shifted to the right or left with respect to portions of sample with higher or lower speed, respectively (44, 45). If there is a discontinuity in the specimen (such as air or any other material with much higher or lower impedance than the specimen), the interference lines at this location will either distort or vanish due to diffraction effects. These types of discontinuities provide contrast in the image.

A small representative region (~3 mm by 6 mm) of the sample was cut out using a razor blade. The real-time interference image of the specimen was displayed on the SLAM's monitor. The sample was magnified by approximately 100×. The field-of-view of the image was approximately 3 mm horizontally by 2 mm vertically. A frame grabber was used to digitize the video signal of the interference images. Eight digitized images per sample were collected, saved in TIFF (tagged image file format) format, and averaged to improve image quality. Each averaged image was improved by histogram equalization to enhance the contrast. Finally, the median filter was applied to remove the speckle noise on the image. All image processing was performed by the Image Processing Toolbox in MATLAB® (The Math Works, Inc., Natick, Mass.)

RESULTS AND DISCUSSION

The BAI-Mode Imaging

Two samples were generated at each sealing-bar temperature. Twenty-four all-plastic and twenty-four foil-containing samples were evaluated. *Figure 3* illustrates the BAI-mode images of all-plastic samples produced at

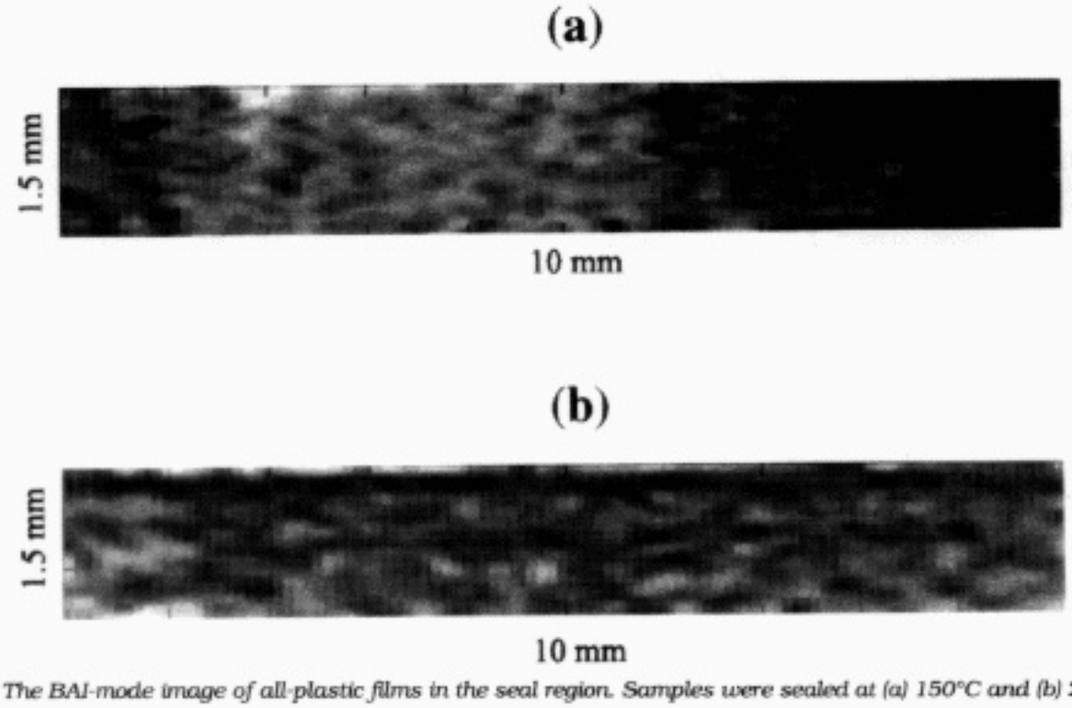

Fig. 3. The BAI-mode image of all-plastic films in the seal region. Samples were sealed at (a) 150°C and (b) 200°C.

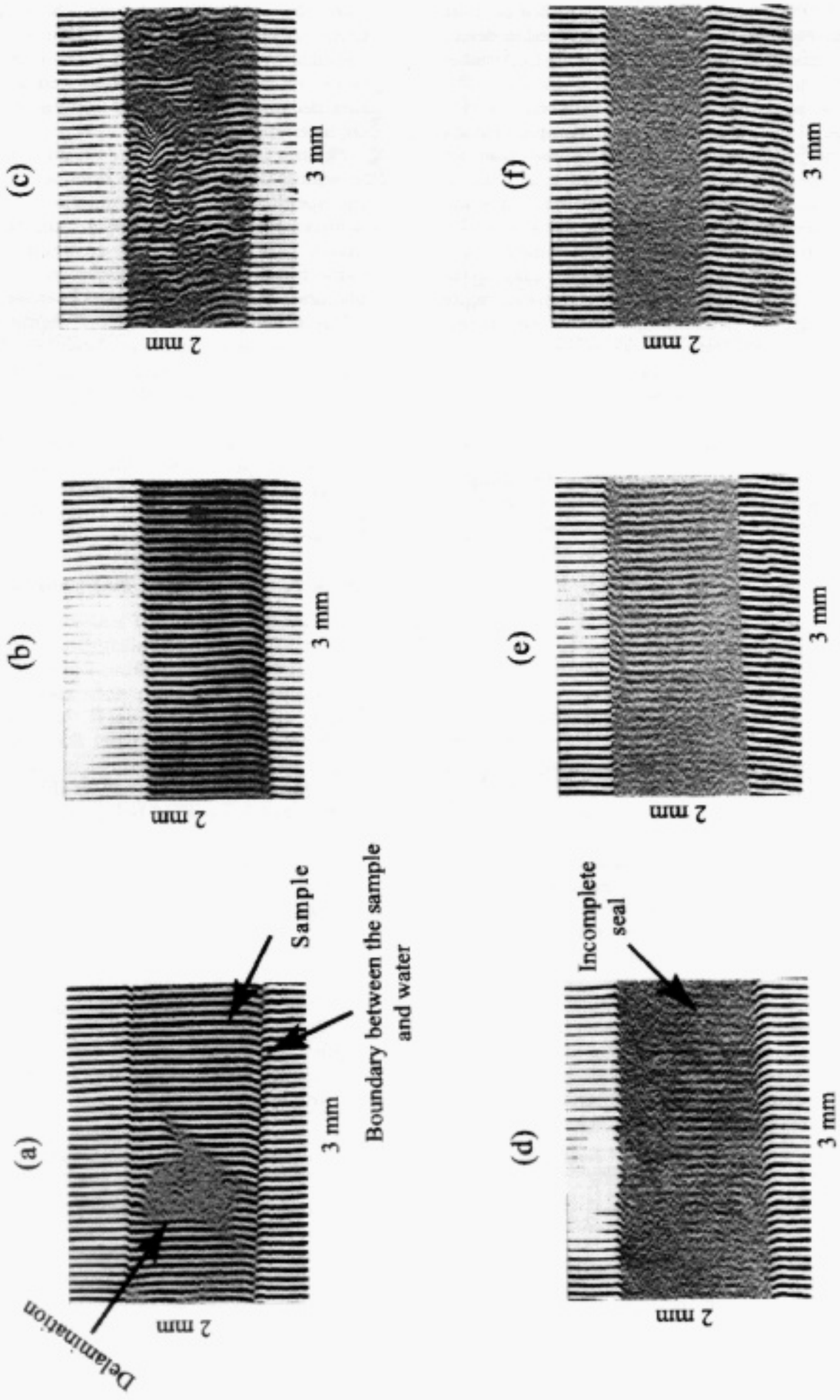

Fig. 4. SLAM interference image of all-plastic samples (a, b, and c) and foil-containing samples (d, e, and f) produced at (a) 90°C, (b) 150°C, (c) 200°C, (d) 150°C, (e) 200°C, and (f) 240°C.

150°C and 200°C. Visual observations indicated that the sample in *Fig. 3a* did not include any visible defect on its surface and that the sample in *Fig. 3b* had visible bubbles and wrinkles on its surface. The BAI-mode images make no apparent distinction between the two samples. Visual examination of other samples established that the BAI-imaging technique by itself was not capable of detecting wrinkles, bubbles and blisters when they were distributed in the seal area. In some samples produced at low sealing-bar temperatures, the layers were separated after they were scanned. However, these samples did not show any discontinuity in the BAI-mode images. The reason for the BAI-mode imaging not detecting delamination while it can detect micro-defects such as channel leaks as small as 6 μm (33, 34) is the insufficient contrast between the defect region and the solid part of the seal.

Sample Validation by SLAM

Figure 4 shows SLAM interference images of samples (three all-plastic samples and three foil-containing samples) constructed at different sealing-bar temperatures. Shifting of interference lines in the boundary between sample and water was observed. The specimen region was always darker than the water region because the ultrasound attenuation coefficient is greater in samples than in water. Interference lines in foil-containing samples were barely visible compared to those in all-plastic samples.

Figures 4a and *d* show SLAM interference images in which the interference lines disappeared in some areas within the sample. This situation was observed in all-plastic and foil-containing samples produced at sealing-bar temperatures ranging from 90 to 120°C and 140 to 170°C, respectively. Some samples exhibited separation of films on completion of the experiment. The interference lines disappear in delaminated or non-bonded regions because the 100-MHz ultrasound does not propagate through these regions because of the layer impedance mismatch between these regions and polymeric materials.

Figures 4b and *e* demonstrate SLAM interference images in which the interference lines were vertically parallel to each other. This pattern of interference lines was seen in all-plastic samples and foil-containing samples created at sealing-bar temperatures ranging from 130 to 170°C and from 180 to 220°C, respectively. A visual inspection of the surfaces of these samples in the seal region showed very smooth surfaces. Thus, seal regions produced at these temperature ranges result in SLAM images with ordered vertical interference lines.

Figures 4c and *f* show the SLAM interference images in which the interference lines are mixed up inside the specimen region. All-plastic and foil-containing samples constructed at the sealing-bar temperatures above 180°C and 230°C, respectively, yielded the same results. Wrinkles, discoloration, bubbles, and blisters were visually observed in these samples.

The sealing-bar temperature regimes have been divided into three categories based on the interference image and visual observations. *Table 1* lists these regimes for each sample group and summarizes the SLAM study. At low sealing-bar temperatures (regime-I), the incomplete seals were created. At optimal sealing-bar temperatures (regime-II), no defects were observed in the seal area. Finally, at high sealing-bar temperatures (regime-II), there were wrinkles and bubbles on the seal surface.

Mean BAI-Value of the BAI-Value Matrix

Figure 5 shows mean BAI-values of samples produced at different sealing-bar temperatures. The mean BAI-values in regimes-I and -III decrease as the sealing-bar temperature increases, and are approximately constant in regime-II. Also, mean BAI-values in regime-I are higher than those in regime-II, and higher in regime-II than those in regime-III.

Regime-I shows the range for the temperature application that is possibly below the melting point of the polymer in the seal area. Incomplete melting causes partial interchain diffusion of the polymer in the seal interface (30). That resulted in post-seal delamination or nonbonding in the seal area of the sample. High mean BAI-values in regime-I suggest that the amplitude of the reflected echo signal is stronger than that in other regimes. Consequently, delamination or nonbonding in the seal causes a greater reflected echo amplitude to return to the transducer because of the higher acoustic-impedance difference between the discontinuous region in the seal and the polymeric package material.

Table 1. Evaluation of Effect of Sealing Bar-Temperature on All-Plastic and Foil-Containing Samples Using SLAM.

Regime	Packaging Material	Sealing-Bar Temperature Range	Observations
I Low sealing-bar temperature range	all-plastic film	90–120°C	SLAM: Interference lines disappeared in non-bonding region
	foil-containing film	140–170°C	Visual: Some samples were delaminated after the data collection
II Optimum sealing-bar temperature range	all-plastic film	130–170°C	SLAM: Smooth vertical interference lines in the specimen area
	foil-containing film	180–220°C	Visual: No visual defect and smooth sample surface
III High sealing-bar temperature range	all-plastic film	180–200°C	SLAM: Interference lines were tangled
	foil-containing film	230–250°C	Visual: Wrinkles, discoloration, bubbles and blisters were clearly visible

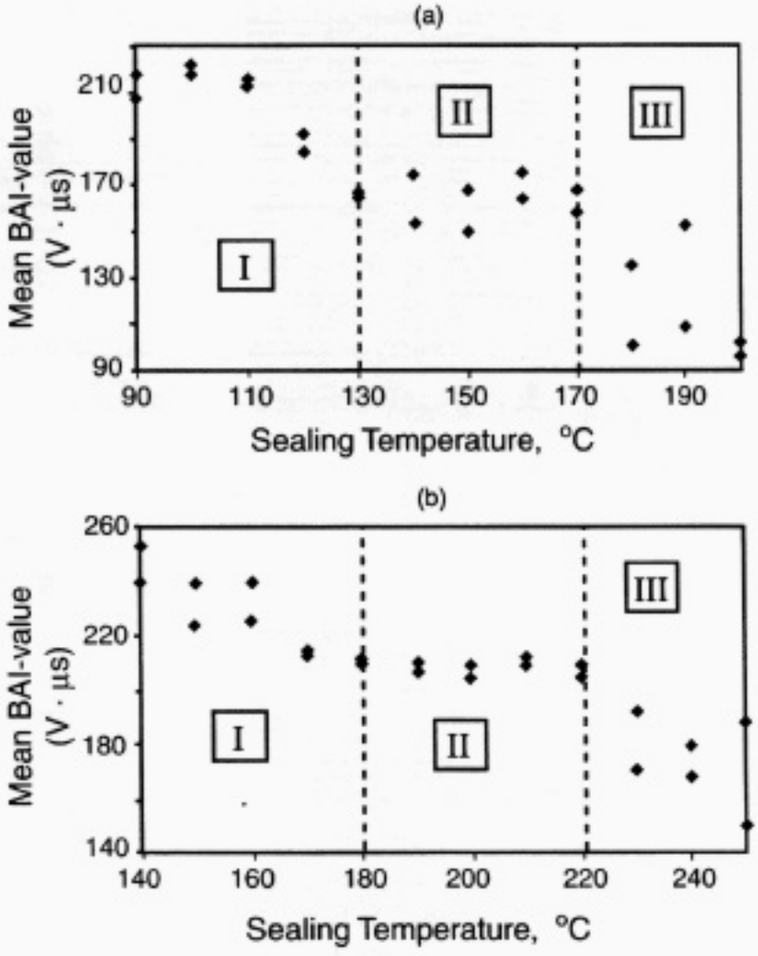

Fig. 5. Mean BAI-values of (a) all-plastic films and (b) foil containing films constructed at different sealing bar temperatures. Dashed lines in the figure separate the three sealing-bar temperature regimes obtained by the SLAM and visual observations.

Regime-III shows the range for temperature application that is far above the melting point of the polymer in the seal interface. Overheating of polymers can bring about chemical reactions such as crosslinking or material degradation (46). In this regime, wrinkles, bubbles, and blisters were visually observed on the seal surface, and interference lines were scrambled. Low mean BAI-values in regime-III imply that the amplitude of the reflected echo signals diminishes. This decrease is surprising because bubbles and wrinkles in the seal area theoretically reflect more energy than homogenous, solid seal. Thus, the BAI-values in regime-III should have been higher than in regime-II. The reason might be attributed to the change of the thickness in the seal region as the sealing temperature increases, which affects the intensity of the reflected echo signals. However, the post-seal thickness of samples was not measured in this study.

Mean BAI-values were uniform in regime-II, ranging from 150 to 175 V·μs and from 205 to 211 V·μs for all-plastic films and foil-containing samples, respectively. The SLAM and visual observations had previously shown that samples produced at the optimum sealing-bar temperature range (regime-II) had very smooth surfaces and that the interference lines were not disturbed. Thus, so long as sealing is performed at optimum conditions, the mean BAI-value of the package seal will not vary significantly in comparison to that for other processing conditions.

Coefficient of Variation of the BAI-Value Matrix (BAICV)

Figure 6 shows the BAICV-values for samples produced at different sealing bar temperatures. The lower the BAICV-values, the smaller the variations in the data, i.e., values in the data are closer to the mean value. The BAICV-values in regime-II (for which defects were not visible on the sample surface) are 10% and 2.5% lower than those in regime-I and regime-III (which had visible bubbles, blisters, and wrinkles) for all-plastic and foil-containing films, respectively. Also, data variation is much higher in regime-III than regime-I because regime-III has a high degree of inhomogeneity due to bubbles and wrinkles with respect to regime-I in which seals are partially welded. Thus, if the seal region of the package contains defects, the variation of the BAI-values in the data is high, and can be measured by calculating the coefficient of variation of the data.

The BAICV-Value Versus Mean BAI-Value

Figure 7 shows the mean BAI- and BAICV-values for each sample. For the all-plastic samples, the mean BAI-values are between 150 and 175 V·μs and the BAICV-values are lower than 10%. This area is regime-II as indicated in *Fig. 7a*. For foil-containing samples, regime-II is bounded by mean BAI-values between 205 and 211 V·μs and BAICV-values lower

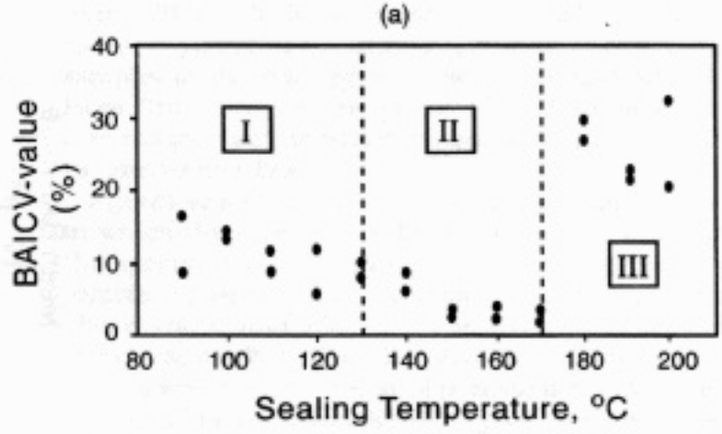

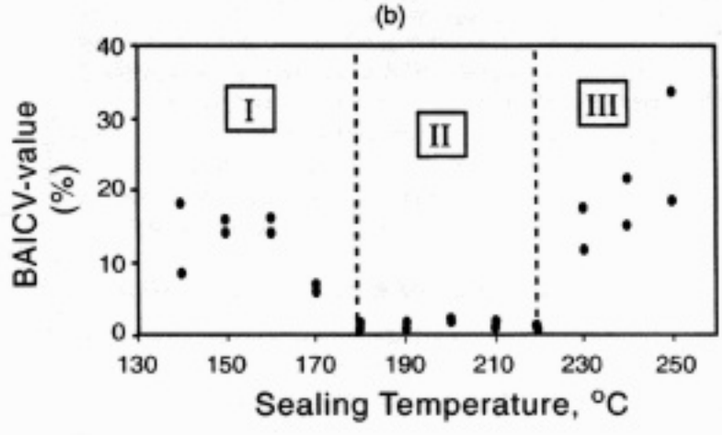

Fig. 6. Coefficient of variation of the BAI-values (BAICV) in the BAI-value matrix for (a) all-plastic films and (b) foil containing films created at different sealing bar temperatures.

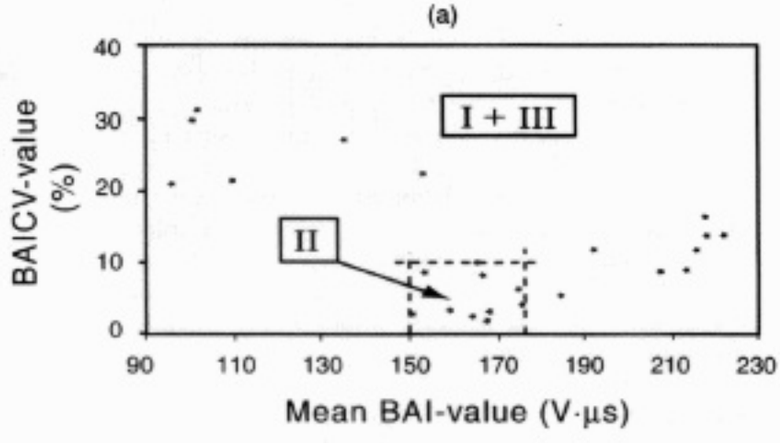

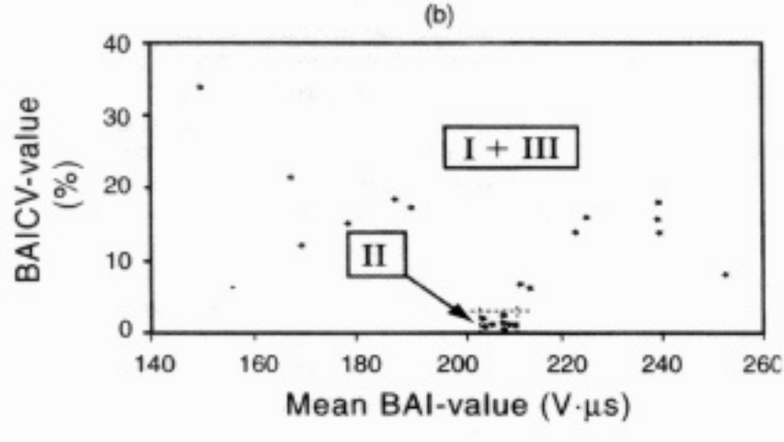

Fig. 7. The BAICV-values versus mean BAI-values for (a) all-plastic films and (b) foil containing films. Data points were collected from Fig. 5 and Fig. 6.

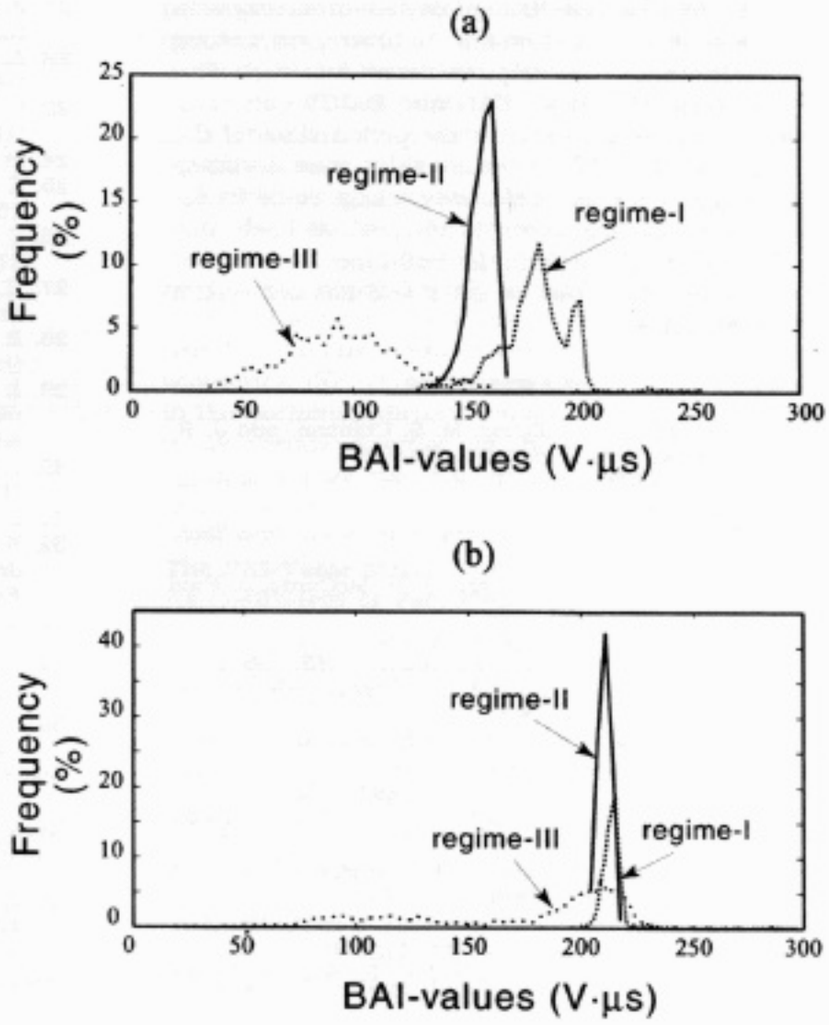

Fig. 8. The frequency distribution of the BAI-values in the seal region of (a) the all-plastic films; (b) the foil-containing films.

than 2.5% as shown in *Fig. 7b*. Other data points in these figures are from regime-I and regime-III. *Figure 7* shows that so long as the package seal contains no defects, its mean BAI-value will not vary much in comparison to package seal containing defects, and its BAICV-value will approach to zero.

Figures 8a and *b* show, respectively, the distribution of the BAI-values in the seal area of the all-plastic and the foil-containing packages. In these figures, the distribution of the BAI-values is shown for each regime. The distribution curve of each regime was drawn by adding all the BAI-values in the same region. For instance, regime-I in *Fig. 8a* includes the BAI-values collected for sealing-bar temperatures between of 90°C and 120°C. From *Fig. 5a*, this regime includes eight BAI-value matrixes. Since each matrix was made up of 750 BAI-values, regime-I in *Fig. 8a* represents the distribution of 6000 BAI-values. As shown in *Fig. 8*, shapes of the distribution curves in regime-I and regime-III are more dispersed than those of regime-II because of the high variation of data. On the other hand, the BAI-values are closer to the mean BAI-value in regime-II, resulting in spike in the distribution curve. To minimize possible formation of defects in an ideal package-sealing operation, the BAI-values should be very close to the mean BAI-value in the seal region, which lowers the BAICV-values.

CONCLUSION

The mean BAI-value and the variation of the BAI-values (BAICV) in the seal region provide an effective way to detect macrodefects such as delamination, non-bonding, wrinkles, blisters, and bubbles that BAI-mode imaging can not detect when there are many defects in the seal area. At optimum sealing conditions, the mean BAI-value of the solid seal is uniform, and the BAICV-value becomes closer to zero. Also, the upper and lower limits for mean BAI- and the BAICV-values for optimum sealing conditions would be different for different packaging materials.

A combination of the mean BAI-value, the BAICV-value, and the BAI-mode imaging can be used for performing a thorough inspection of package seals. The mean BAI-value and the BAICV-value can be used to detect macroscale seal defects and BAI-mode image can be used to detect microscopic defects. When macroscale defects are detected by the inspection system, further testing for microscopic defects is not required, thereby decreasing inspection time and cost.

The target of an effective quality assurance system must be to detect faults on line. In this regard, testing sealer performance will improve the on-line inspection of packages. The mean BAI- and BAICV-values of seals can be used to predict the performance of the sealing operation. When these values start deviating from acceptable levels, defective package could be rejected, and machine setting is adjusted. As such, this method offers the potential for real-time, on-line control by sensing whether or not a seal has achieved a proper fusion state.

REFERENCES

1. J. F. Steffe, J. R. Williams, M. S. Chinnan, and J. R. Black, *Food Technology*, **34(9)**, 39 (1980).
2. A. F. Badenhop and H. P. Milleville, *Food Processing*, **44**, 82 (1980).
3. J. R. Williams, J. F. Steffe, and J. R. Black, *Food Technology*, **37**, 92 (1983).
4. P. J. Delaquis, R. Baker, and A. R. McCurdy, *J. Food Protection*, **49(1)**, 42 (1986).
5. C. E. Morris, *Food Eng.*, **2**, 44 (1989).
6. R. A. Lampi, in *Advance Food Research*, **23**, 305, C. O. Chichester, E. M. Mark, and G. F. Stewart, eds., Academic Press, New York (1977).
7. J. P Adams, W. R. Peterson, and W. S. Otwell, *Food Technology*, **37**, 123 (1983).
8. A. E. Sloan, *Food Engineering*, **57**, 48 (1985).
9. T. D. Durance and L. S. Collins, *J. Food Science*, **56(5)**, 1282 (1991).
10. R. A. Kluter, D. T. Nattress, C. P. Dunne, and R. D. Popper, *J. Food Science*, **59(4)**, 849 (1994).
11. H. M. C. Put, H. Van Doren, W. R. Warner, and J. T. Kruiswjik, *J. Appl. Bacteriol.*, **35**, 7 (1972).
12. H. M. C. Put, W. R. Witvoet, and W. R., Warner, *J. Food Protection*, **43**, 488 (1980).
13. R. Ahvenainen, *Food Rev.*, **4(1)**, 45 (1988).
14. S. McEldowney and M. Fletcher, *J. Appl. Bacteriol.*, **69**, 190 (1990).
15. C. L. Harper, in *Plastic Package Integrity Testing Assuring Seal Quality*, **C10**, 79, B. A. Blakistone and C. L. Harper, ed., Institute of Packaging Professionals, Herndon, Va. (1995).
16. Flexible Package Integrity Committee of the National Food Processors Association, *Flexible Package Integrity Bulletin*, NFPA Bulletin 41-L, NFPA, Washington, D.C. (1989).
17. D. Warrick, *Food Manufac.*, **65(10)**, 63 (1990).
18. C. L. Harper, B. S. Blakistone, J. B. Litchfield, and S. A. Morris, *Food Technology*, **6(10)**, 336 (1995).
19. V. K. Stokes, *Polym. Eng. Sci.*, **28**, 718 (1988).
20. V. K. Stokes, *Polym. Eng. Sci.*, **28**, 728 (1988).
21. A. Benatar, R. V. Eswaran, and S. K. Nayar, *Polym. Eng. Sci.*, **29**, 1689 (1989).
22. A. Benatar and Z. Cheng, *Polym. Eng. Sci.*, **29**, 1699 (1989).
23. H. Potente and J. Natrop, *Polym. Eng. Sci.*, **31**, 519 (1991).
24. M. C. Gabriele, *Plastics Technology*, **39(4)**, 53 (1993).
25. C. J. Nonhof and G. A. Loiten, *Polym. Eng. Sci.*, **34**, 1547 (1994).
26. C. J. Nonhof and G. A. Luiten, *Polym. Eng. Sci.*, **36**, 1177 (1996).
27. H. V. Wijk, G. A. Luiten, and P. G. V. Engen, *Polym. Eng. Sci.*, **36**, 1165 (1996).
28. H. J. Yeh and A. Benatar, *TAPPI Journal*, **80(6)**, 197 (1997).
29. H. S. Kaufman and J. J. Falcetta, *Introduction to Polymer Science and Technology: An SPE Textbook*, John Wiley & Sons, New York (1977).
30. D. B. Kline and R. P. Wool, *Polym. Eng. Sci.*, **28**, 52 (1988).
31. J. Nieh and L. J. Lee, *Polym. Eng. Sci.*, **38**, 1121 (1998).
32. K. Raum, A. Ozguler, S. A. Morris, and W. D. O'Brien, Jr., *IEEE Transactions on Ultrasonics, Ferroelectrics, and Frequency Control*, **45(1)**, 30 (1998).
33. A. Ozguler, S. A. Morris, and W. D. O'Brien, Jr., *J. Food Science*, **63(4)**, 673 (1998).
34. A. Ozguler, S. A. Morris, and W. D. O'Brien, Jr., *Packaging Technology & Science*, **12(4)**, 161 (2000).
35. S. A. Morris, A. Ozguler, and W. D. O'Brien, Jr., *Packaging Technology & Engineering*, **7(7)**, 42 (1998).
36. S. A. Morris, A. Ozguler, and W. D. O'Brien, Jr., *Packaging Technology & Engineering*, **7(8)**, 52 (1998).
37. C. H. Frazier, A. Ozguler, S. A. Morris, and W. D. O'Brien, Jr., *IEEE Transactions on Ultrasonics, Ferroelectrics, and Frequency Control*, **47(3)**, 530 (2000).
38. Q. Tian, B. Sun, A. Ozguler, S. A. Morris, and W. D. O'Brien, Jr., *IEEE Transactions on Ultrasonics, Ferroelectrics, and Frequency Control*, **47(3)**, 635 (2000).
39. K. Raum and W. D. O'Brien, Jr., *IEEE Transactions on Ultrasonics, Ferroelectrics and Frequency Control*, **44(4)**, 810 (1997).
40. W.D. Wilson, *J. Acoust. Soc. Amer.*, **31**, 1067 (1959).
41. A. A. Safvi, H. J. Meerbaum, S. A. Morris, C. L. Harper, and W. D. O'Brien, Jr., *J. Food Protection*, **60(3)**, 309 (1996).
42. A. Briggs, *An Introduction to Scanning Acoustic Microscopy*, Oxford University Press, Oxford, England (1985).
43. A. Briggs, *Acoustic Microscopy*, Clarendon Press, Oxford, England (1992).
44. W. D. O'Brien, Jr., *J. the Acoust. Soc. of Amer.*, **69(2)**, 575 (1981).
45. P. M. Embree, S. G. Foster, G. Bright, and W. D. O'Brien, Jr., *Acoustic Imaging*, **13**, 203 (1984).
46. L. E. Nielsen, *Mechanical Properties of Polymers*, Chapman & Hall, Ltd., London (1962).